Scripta Materialia 142 (2018) 79–82

Contents lists available at ScienceDirect

Scripta Materialia

journal homepage: www.elsevier.com/locate/scriptamat

Regular article

Water-assisted flash sintering: Flashing ZnO at room temperature to achieve ~98% density in seconds

Jiuyuan Nie, Yuanyao Zhang, Jonathan M. Chan, Rongxia Huang, Jian Luo *

Department of NanoEngineering, University of California, San Diego, La Jolla, CA 92093, USA

ARTICLE INFO

Article history:
Received 24 July 2017
Received in revised form 17 August 2017
Accepted 18 August 2017
Available online xxxx

Keywords:
Flash sintering
Water-assisted sintering
Ultrafast densification
Energy-saving ceramic fabrication
ZnO

ABSTRACT

Water can trigger flash sintering of ZnO powder pellets at room temperature to achieve ~98% of the theoretical density in 30 s without any external furnace heating. The specimen conductivity can be increased by >10,000 times *via* absorbing water vapor to enable the room-temperature flash. The initial electric field must be higher than a critical threshold to lead to densification, suggesting bifurcation in kinetic pathways. This new cost and energy saving water-assisted flash sintering (WAFS) technology can potentially be applied to consolidate other ceramic materials.

On one hand, Raj and co-workers reported an innovative "flash sintering" technology in 2010 to use applied electric fields/currents to trigger fast densification at low furnace temperatures [1], which has been successfully applied to a broad range of ceramics [1–15] (as being recently reviewed by Yu et al. [16]). Low furnace temperatures and fast densification rates make flash sintering an energy-saving and cost-effective method to consolidate ceramics. A further pursuit of even lower onset flash temperatures was made by increasing the initial applied electric field ($E_{initial}$); specifically, the onset flash temperature of 8 mol% Y_2O_3 stabilized ZrO_2 was lowered to 390 °C with a high $E_{initial}$ of 2250 V/cm [17], but only moderate densification (*i.e.*, ~8.5% linear shrinkage) was achieved [17]. Another prior work demonstrated that a reduced atmosphere (Ar + 5% H_2) can significantly lower the flash temperature of ZnO to <120 °C (*via* increasing the specimen conductivity to trigger a thermal runaway at a lower temperature, as supported by a quantitative model [4,5,18]) with an applied $E_{initial}$ of 500 V/cm [18]. Yet, a further reduction of the flash temperature could not be achieved (*e.g.*, even with a higher $E_{initial}$ of 1000 V/cm [18]), presumably because the reduced atmosphere cannot interact with the specimen effectively at <100 °C. Thus, a scientifically-interesting and technologically-attractive goal of triggering the flash sintering at room temperature without any external furnace heating has remained unattainable, which motivated the current study.

On the other hand, ceramic researchers have observed enhanced or suppressed sintering rates of MgO [19], CaO [20], anatase TiO_2 [21], SnO_2 [22], ZnO [23], and doped Al_2O_3 [24] in the presence of water vapor. Recently, Randall and co-workers developed an innovative "cold sintering process (CSP)" to densify ceramics under 250 °C with the assistance of water or aqueous solutions under the pressure of several hundreds of MPa [25,26], which has been successfully applied to $BaTiO_3$ [27], ZrO_2 [28,29], ZnO [30], $NaNO_2$ and KH_2PO_4 [31], and V_2O_5 based ceramic-polymer composites [32]. Moreover, Guillon and co-workers recently discovered enhanced densification by adding water in nanocrystalline ZnO specimens sintered by the spark plasmas sintering/field-assisted sintering technology (SPS/FAST) [33,34].

The above inspiring studies on electric field/current and water assisted sintering collectively motivated us to propose, and subsequently validate with experiments on the ZnO model system, a new water-assisted flash sintering (WAFS) method. In this study, we demonstrated that WAFS can reduce the onset flash of the ZnO powder specimen to room temperature and subsequently achieve ~98% of the theoretical density in 30 s.

A >99.99% purity ZnO powder, purchased from Sigma Aldrich, was mixed with 0.5 wt% binder (2 wt% PVA in DI water), uniaxially pressed at ~300 MPa to form green pellets of D (diameter) = 6.4 mm and H (height) = 1.0 mm, and subsequently baked at 500 °C for 1 h to burn out the binder. The average grain sizes in the green pellets were measured to be ~120 nm, and the relative densities were measured to be 54.8 ± 0.4%. The Pt electrodes were sputtered on both sides of surfaces and specimens were loaded into a horizontal quartz tube to connect with a Pt/Cu wire system (that has a negligible total resistance as compared with that of the ZnO specimen under all experimental conditions) for applying electric fields/currents. Flash sintering experiments were conducted in wet Ar + 5 mol% H_2, by flowing the gas through a conical flask containing DI water at room temperature (as schematically shown

* Corresponding author.
E-mail address: jluo@alum.mit.edu (J. Luo).

http://dx.doi.org/10.1016/j.scriptamat.2017.08.032
1359-6462/

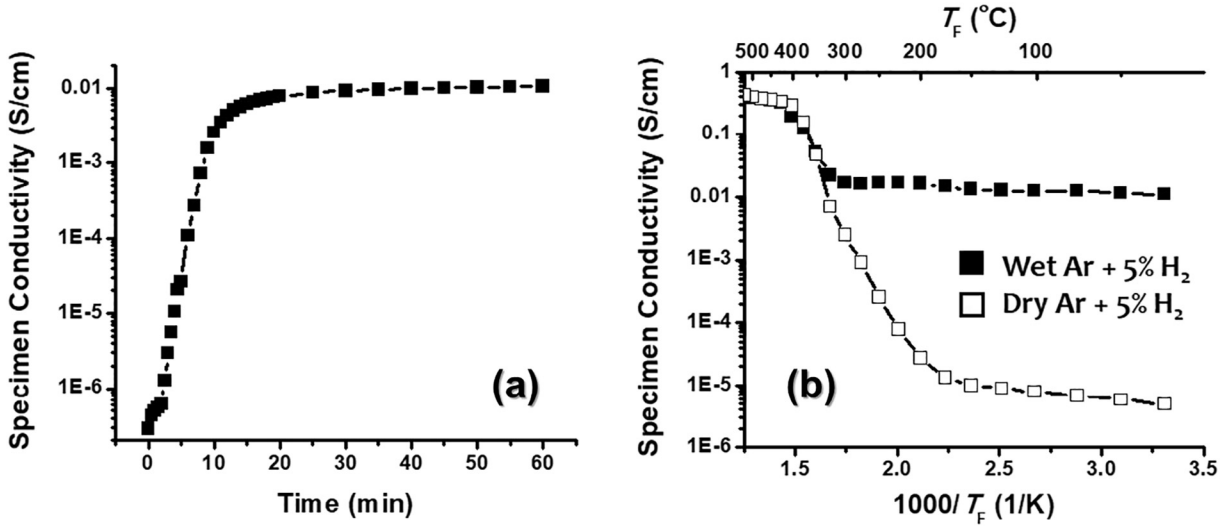

Fig. 1. (a) Specimen conductivity *vs.* time curve of a ZnO green pellet in flowing wet Ar + 5% H_2. (b) Specimen conductivity *vs.* temperature curves measured from two ZnO specimens in dry and wet Ar + 5% H_2, respectively, in a furnace that was heated at a constant ramping rate of 20 °C/min.

in the graphical abstract). The system was purged with the flowing wet gas for 1 h before conducting flash sintering experiments. The specimen resistance was recorded during this period using a multimeter (DMM 4050, Tektronix Inc.). Subsequently, the flash sintering experiments were conducted at room temperature using a DC power supply (Sorensen XHR 150-7, Ametek Programmable Power Inc.) with initial electric fields $E_{initial}$ = 200, 150, and 100 V/cm, respectively. The power supply was automatically switched to a current-control mode after the flash once the current reached a preset maximum current of I_{max} = 2.4 A (corresponding to a nominal current density of $J \approx 75$ mA/mm^2, calculated without considering the densification of the specimen) for all flash sintering experiments. The electric power supply was shut off 30 s after the onset of flash sintering. Specimen densities were measured by the Archimedes method (for dense specimens) and/or *via* measuring the dimension and weight. The microstructures were characterized using a field emission scanning electron microscope (FE SEM, Philips XL30). Grain sizes were measured from polished specimens using a standard intercept method.

Fig. 1 (a) shows the specimen conductivity *vs.* time curve of a ZnO green pellet after flowing with wet Ar + 5% H_2. The specimen conductivity increased steeply by more than four orders of magnitude from ~3×10^{-7} S/cm to ~7×10^{-3} S/cm in the first ~20 min after purging with the wet gas, presumably due to water absorption, and reached a steady state, approaching ~0.01 S/cm. To further understand the effects of absorbed water, we conducted an additional experiment to measure the conductivities of ZnO powder pellets in both dry and wet flowing Ar + 5% H_2 in a tube furnace with a constant heating rate of 20 °C/min (after first flowing for 1 h at room temperature to achieve the steady state). It is interesting to note from Fig. 1(b) that the conductivity of the specimen in wet flowing gas was almost constant and higher than

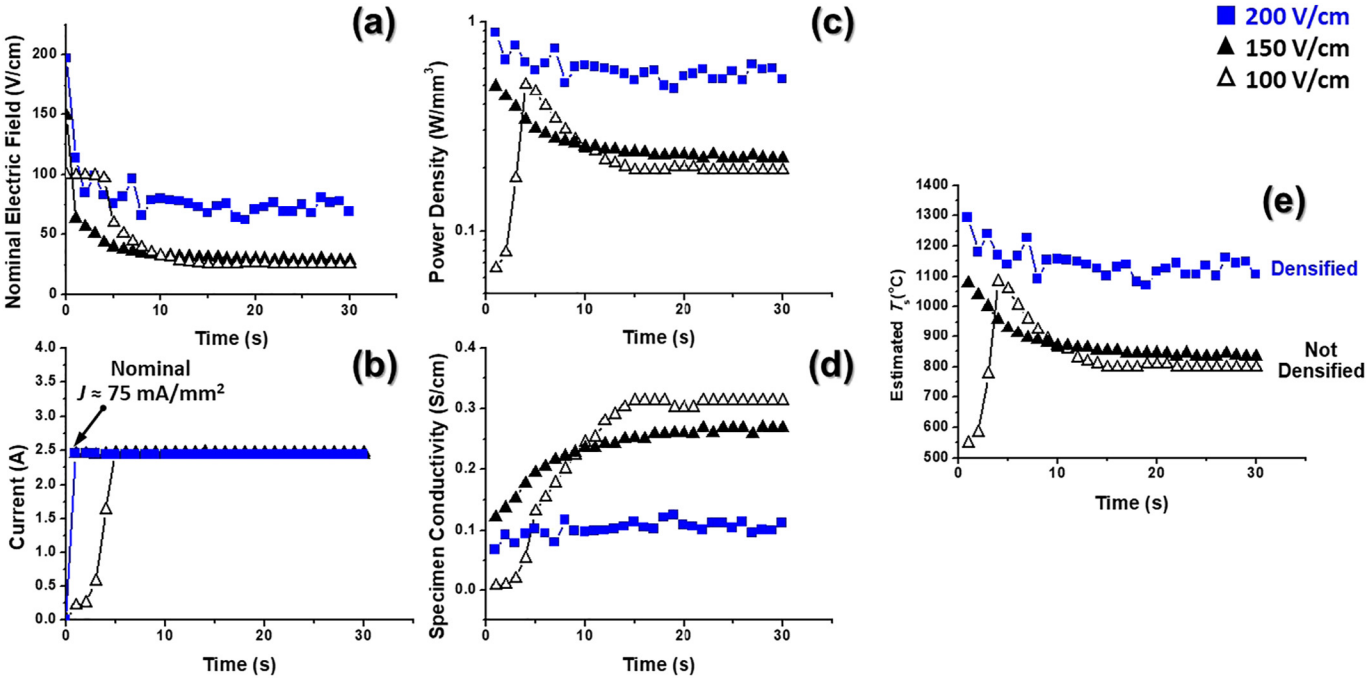

Fig. 2. The (a) nominal electric field, (b) current, (c) power density, (d) specimen conductivity, and (e) estimated specimen temperature (T_S) of ZnO *vs.* time curves during water-assisted flash sintering (WAFS) of three ZnO specimens with $E_{initial}$ = 100, 150, and 200 V/cm.

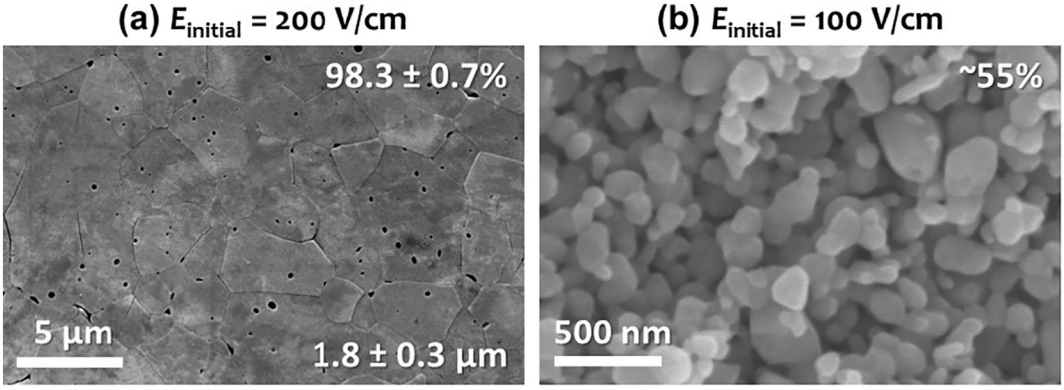

Fig. 3. SEM micrographs of (a) a polished cross section of a flash-sintered ZnO specimen with $E_{initial}$ = 200 V/cm and (b) a fractured surface of a specimen with $E_{initial}$ = 100 V/cm.

that of the dry specimen until ~350 °C, at which temperature the conductivity of the dry specimen increased to the same level. This suggests that the water effects can persist at least to ~350 °C in the powder specimen at the heating rate of 20 °C/min and probably to even higher temperatures with two to three orders of magnitude higher heating rates in flash sintering [5], which may help sustain the WAFS after the onset of a flash.

Fig. 2 shows the electric fields, currents, power densities, specimen conductivities, and estimated specimen temperatures (T_S) from a blackbody radiation model [4] during 30 s of the WAFS of three ZnO specimens with the initial electric field of $E_{initial}$ = 100, 150, and 200 V/cm, respectively. At the low $E_{initial}$ of 100 V/cm, a flash started gradually after an incubation period of ~5 s; at the intermediate $E_{initial}$ of 150 V/cm, a flash started intermediately. In both cases, the power densities (Fig. 2(c)) and estimated specimen temperatures (Fig. 2(e)) first increased but subsequently dropped to steady states, which were due to the increasing specimen conductivities (Fig. 2(d)) that generated less power in the constant-current mode. Consequently, the specimens reached the steady-state temperatures of 800–900 °C after ~10 s in these two cases, which did not lead to substantial densification/sintering. In contrast, with a high $E_{initial}$ = 200 V/cm, the power density immediately reached, and subsequently sustained at, a higher level of ~0.6 W/mm^3 to sustain the specimen temperature at >1100 °C (Fig. 2(e)) to enable fast densification. Consistently, the specimen with $E_{initial}$ = 200 V/cm achieved ~98.3 ± 0.7% relative density after WAFS for 30 s with a measured average grain size of 1.83 ± 0.30 μm (Fig. 3(a)). The observed pores trapped inside large grains (Fig. 3(a)) are evidence of rapid grain growth during the flash sintering that led to pore-boundary separation. In contrast, the specimens with $E_{initial}$ = 100 V/cm and 150 V/cm essentially did not densify/sinter appreciably (Fig. 3(b)) because of the lower steady-state specimen temperature of ~850 °C (Fig. 2(e)).

The observation that densification only occurred when the $E_{initial}$ was above a critical threshold (Fig. 2 and Fig. 3) suggested the existence of bifurcation [35] in kinetic pathways after the flash events. In other words, the final steady states set (constrained) by the preset experimental condition of I_{max} = 2.4 A can be satisfied by two specimen states: a low-temperature (~850 °C) un-sintered (powder) specimen with a higher conductivity (~0.3 S/cm, which is presumably due to high surface conductivity) *vs.* a high-temperature (~1100 °C) sintered specimen with lower bulk conductivity (~0.1 S/cm). When $E_{initial}$ was sufficiently high (*e.g.*, 200 V/cm), the high initial power generation and the associated high heating rate led to the densification pathway and latter state of a dense, bulk specimen; otherwise, the specimen would remain un-sintered (as a powder specimen with high surface conduction) at the lower $E_{initial}$ of 100 or 150 V/cm.

The exact role of water in assisting densification of ZnO is not yet clear. In addition to triggering the flash at room temperature by substantially increasing the specimen conductivity, water could also help the mass transport as demonstrated by the water assisted SPS/FAST of ZnO that was substantial at ~250–400 °C [33,34]. The water effects on transport could be effective in the initial stage of WAFS (before drying); Fig. 1(b) suggests that the water effects can persist to at least ~350 °C at the heating rate of 20 °C/min and they can persist to higher temperatures during flash sintering where the heating rate is on the order of 100 °C/s [5]; furthermore, such effects can be more pronouncing with a high $E_{initial}$ that leads to extremely high initial heating and densification rates. Nonetheless, it is still difficult to determine how significant the water in fact enhanced the mass transport of ZnO, if any, in the current case of WAFS. Furthermore, we recognize that the reduced atmosphere (wet Ar + 5% H_2) plays an important role to enable and/or sustain flash sintering *via* reduction of ZnO during the sintering (probably after the room-temperature flash). While water can substantially increase the conductivities of many green specimens at room temperature, studies are currently being conducted to investigate the applicability of this WAFS method to other ceramic materials.

In summary, a new WAFS method was proposed for the first time. Using ZnO as a model system, this study successfully demonstrated that WAFS can start at room temperature to achieve ~98% relative density in 30 s in wet Ar + 5% H_2. This method can potentially be extended to consolidate other ceramic systems to achieve fast densification at extremely low furnace temperatures or, ideally, room temperature. Furthermore, this study suggests significant technological opportunities for energy and cost savings *via* exploiting and investigating new ceramic processing science through the interplay of water, electric fields/currents, and ultrafast heating rates.

This work is supported by the Aerospace Materials for Extreme Environments program of the U.S. Air Force Office of Scientific Research (AFOSR) under the grant no FA9550-14-1-0174. We gratefully thank our AFOSR program manager, Dr. Ali Sayir, for his support and guidance.

References

[1] M. Cologna, B. Rashkova, R. Raj, J. Am. Ceram. Soc. 93 (2010) 3556–3559.
[2] M. Cologna, A.L. Prette, R. Raj, J. Am. Ceram. Soc. 94 (2011) 316–319.
[3] H. Yoshida, Y. Sakka, T. Yamamoto, J.-M. Lebrun, R. Raj, J. Eur. Ceram. Soc. 34 (2014) 991–1000.
[4] Y.Y. Zhang, J.I. Jung, J. Luo, Acta Mater. 94 (2015) 87–100.
[5] Y.Y. Zhang, J.Y. Nie, J.M. Chan, J. Luo, Acta Mater. 125 (2017) 465–475.
[6] C. Schmerbauch, J. Gonzalez-Julian, R. Röder, C. Ronning, O. Guillon, J. Am. Ceram. Soc. 97 (2014) 1728–1735.
[7] Y.Y. Zhang, J.Y. Nie, J. Luo, J. Ceram. Soc. Jpn. 124 (2016) 296–300.
[8] S.K. Jha, R. Raj, J. Am. Ceram. Soc. 97 (2014) 527–534.
[9] A. Karakuscu, M. Cologna, D. Yarotski, J. Won, J.S. Francis, R. Raj, B.P. Uberuaga, J. Am. Ceram. Soc. 95 (2012) 2531–2536.
[10] A. Gaur, V.M. Sglavo, J. Mater. Sci. 49 (2014) 6321–6332.
[11] A.L. Prette, M. Cologna, V. Sglavo, R. Raj, J. Power, Sources 196 (2011) 2061–2065.
[12] E. Zapata-Solvas, S. Bonilla, P. Wilshaw, R. Todd, J. Eur. Ceram. Soc. 33 (2013) 2811–2816.
[13] S. Grasso, T. Saunders, H. Porwal, B. Milsom, A. Tudball, M. Reece, J. Am. Ceram. Soc. (2016).
[14] S. Grasso, T. Saunders, H. Porwal, O. Cedillos-Barraza, D.D. Jayaseelan, W.E. Lee, M.J. Reece, J. Am. Ceram. Soc. 97 (2014) 2405–2408.
[15] J. Nie, Y. Zhang, J.M. Chan, S. Jiang, R. Huang, J. Luo, Scr. Mater. 141 (2017) 6–9.

[16] M. Yu, S. Grasso, R. McKinnon, T. Saunders, M.J. Reece, Adv. Appl. Ceram. 116 (2017) 24–60.
[17] J.A. Downs, V.M. Sglavo, J. Am. Ceram. Soc. 96 (2013) 1342–1344.
[18] Y.Y. Zhang, J. Luo, Scr. Mater. 106 (2015) 26–29.
[19] P.J. Anderson, P.L. Morgan, Trans. Faraday Soc. 60 (1964) (930-&).
[20] R.H. Borgwardt, Ind. Eng. Chem. Res. 28 (1989) 493–500.
[21] J.L. Hebrard, P. Nortier, M. Pijolat, M. Soustelle, J. Am. Ceram. Soc. 73 (1990) 79–84.
[22] L. Perazolli, J.A. Varela, E.R. Leite, E. Longo, Adv. Powder Tech. 299-3 (1999) 134–140.
[23] J.A. Varela, O.J. Whittemore, E. Longo, Ceram. Int. 16 (1990) 177–189.
[24] J.P. Angle, P.E.D. Morgan, M.L. Mecartney, J. Am. Ceram. Soc. 96 (2013) 3372–3374.
[25] J. Guo, S.S. Berbano, H.Z. Guo, A.L. Baker, M.T. Lanagan, C.A. Randall, Adv. Funct. Mater. 26 (2016) 7115–7121.
[26] J. Guo, H.Z. Guo, A.L. Baker, M.T. Lanagan, E.R. Kupp, G.L. Messing, C.A. Randall, Angew. Chem. Int. Ed. 55 (2016) 11457–11461.
[27] H.Z. Guo, A. Baker, J. Guo, C.A. Randall, ACS Nano 10 (2016) 10606–10614.
[28] H.Z. Guo, T.J.M. Bayer, J. Guo, A. Baker, C.A. Randall, J. Eur. Ceram. Soc. 37 (2017) 2303–2308.
[29] H.Z. Guo, J. Guo, A. Baker, C.A. Randall, J. Am. Ceram. Soc. 100 (2017) 491–495.
[30] S. Funahashi, J. Guo, H.Z. Guo, K. Wang, A.L. Baker, K. Shiratsuyu, C.A. Randall, J. Am. Ceram. Soc. 100 (2017) 546–553.
[31] H.Z. Guo, A. Baker, J. Guo, C.A. Randall, J. Am. Ceram. Soc. 99 (2016) 3489–3507.
[32] J. Guo, H.Z. Guo, D.S.B. Heidary, S. Funahashi, C.A. Randall, J. Eur. Ceram. Soc. 37 (2017) 1529–1534.
[33] B. Dargatz, J. Gonzalez-Julian, M. Bram, P. Jakes, A. Besmehn, L. Schade, R. Roder, C. Ronning, O. Guillon, J. Eur. Ceram. Soc. 36 (2016) 1207–1220.
[34] B. Dargatz, J. Gonzalez-Julian, M. Bram, Y. Shinoda, F. Wakai, O. Guillon, J. Eur. Ceram. Soc. 36 (2016) 1221–1232.
[35] J.G.P. da Silva, H.A. Al-Qureshi, F. Keil, R. Janssen, J. Eur. Ceram. Soc. 36 (2016) 1261–1267.